RESEARCH ARTICLE

Macromolecular Bioscience
www.mbs-journal.de

Early Stage UV-B Induced Molecular Modifications of Human Eye Lens γD-Crystallin

*Susanne Weininger, Malte Neudorf, Stefan Gröger, Eric Plato, Robert Broneske, Kay Saalwächter, Ulrich Weininger, and Jochen Balbach**

In the human eye lenses, the crystallin proteins facilitate transparency, light refraction, as well as UV light protection. A deregulated balanced interplay between α-, β-, and γ-crystallin can cause cataract. γD-crystallin (hγD) is involved in the energy dissipation of absorbed UV light by energy transfer between aromatic side chains. Early UV-B induced damage of hγD with molecular resolution is studied by solution NMR and fluorescence spectroscopy. hγD modifications are restricted to Tyr 17 and Tyr 29 in the N-terminal domain, where a local unfolding of the hydrophobic core is observed. None of the tryptophan residues assisting fluorescence energy transfer is modified and hγD is remained soluble over month. Investigating isotope-labeled hγD surrounded by eye lens extracts from cataract patients reveals very week interactions of solvent-exposed side chains in the C-terminal hγD domain and some remaining photoprotective properties of the extracts. Hereditary E107A hγD found in the eye lens core of infants developing cataract shows under the here used conditions a thermodynamic stability comparable to the wild type but an increased sensitivity toward UV-B irradiation.

1. Introduction

The majority of the protein content of mammalian eye lenses belongs to two superfamilies: α-crystallins, which are small heat shock proteins and βγ−crystallins containing two double Greek key motifs. As there is no metabolic protein turnover in the lens, the crystallins need to remain intact and soluble throughout the human lifespan in order to facilitate a transparent eye lens with sufficient refractive power accomplished by protein concentrations up to 400 mg mL^{-1}.[1] Aggregation and deposition of crystallins becoming insoluble are the world leading cause of blindness due to cataract.[2] Among the α-, β-, and γ-crystallins, the human γD-crystallin (hγD) is predominantly found in the lens nucleus and involved in both age- and inheritance-related cataract.[3] It comprises two domains with a structural Greek-key motif harboring a set of aromatic residues involved in photoprotection.[4] The latter is required to effectively prevent damage of the eye lens from the ambient UV light exposure until old age. Although the corona filters out most of UV radiation of wavelengths shorter than 295 nm,[5] photochemical reaction products especially of tryptophan residues accumulate and increase the risk of cataract formation with time.[6–8]

The main property of the complex mixture of 20 different crystallins in the human eye lens is to avoid aggregation under the very high natural protein concentrations. In this context, α-, β-, and γ-crystallins are structural proteins, while α-crystallins additionally function as molecular chaperones.[4] A well-balanced ratio of all three family members is crucial for a transparent and long-term stable highly concentrated protein solution. Several mechanisms toward imbalances and subsequent opacity have been discussed including liquid–liquid phase separation, UV damage, or amyloid fibril formation.[1] The most common surgery in the world is the removal of the eye lens of cataract patients and the vast majority represent age-related cataract.[2]

The photoprotective mechanism of hγD from UV-B damage (290–320 nm wave lengths) includes an energy transfer from excited Trp 43 to Trp 69 in the N-terminal and from Trp 131 to Trp 157 in the C-terminal domain (**Figure 1**). This energy dissipation finally ends up via backbone amides to surrounding water molecules.[8] Interdomain quenching has almost no contribution to this energy transfer and a very similar interplay of Trp residues had been revealed for human γS-crystallin.[9] During these processes, photoreactive species might detour toward irreversible chemical reactions including oxidation and covalent aromatic bonds to neighboring residues.[7,10,11]

Additionally, more than 20 hereditary point mutations had been identified to cause cataract with different manifestations and time courses of lens opacity., e.g., the W43R variant in the N-terminal domain was found in nuclear congenital cataract of

S. Weininger, M. Neudorf, S. Gröger, E. Plato, R. Broneske, K. Saalwächter, U. Weininger, J. Balbach
Martin Luther University Halle-Wittenberg
Institute of Physics
Betty-Heimann-Strasse 7, DE-06120 Halle, Germany
E-mail: jochen.balbach@physik.uni-halle.de

The ORCID identification number(s) for the author(s) of this article can be found under https://doi.org/10.1002/mabi.202200526

DOI: 10.1002/mabi.202200526

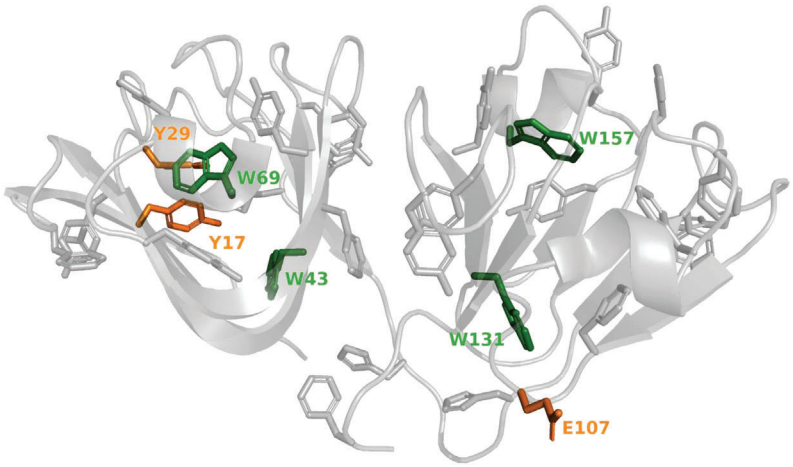

hγD variant
Y17A
Y17AY29A
Y29A
W43R
W69A
E107A
W131A
W157A

Figure 1. W43–W69 and W131–157 FRET pairs (green) of the N- and C-terminal domain of hγD crystallin surrounded by Phe, Try, and His residues (gray, orange) (PyMol illustration of 2klj.pdb). Substituted residues of here studied variants are colored in green and orange and listed on the right.

infants,[12,13] which reduces the thermodynamic stability of hγD without causing significant tertiary structural modifications.[14,15] This variant shows increased oxidative damage by forming covalent disulfide bonds and has been discussed as mimic of UV-C modified hγD causing an increased susceptibility for aggregation.[12,14] There is controversy in the literature whether W43R itself decreases solubility.[12,14] E107A hγD was found in the turbid lens nucleus of children without influencing the thermodynamic stability and secondary structure.[16,17] It had been proposed that its increased isoelectric point and thus increased positive surface charge at physiological pH changed the electrostatic interaction toward E107A hγD itself and α-crystallins driving LLPS and light scattering.[16]

The aim of the here presented study was to identify with molecular resolution, which aromatic residues of hγD get modified at an early stage upon UV-B irradiation using high resolution protein NMR spectroscopy. We find that Tyr 17 and Tyr 29 are the main target of irreversibly modified but still soluble hγD causing a local unfolding in the hydrophobic core of the N-terminal domain. Disease-related W43R hγD showed wild type UV-B sensitivity whereas the E107A variant revealed a higher UV-B sensitivity. Further, we found that eye lens extracts from cataract patients can still protect to some extend the UV-B induced hγD modifications. Mainly solvent-exposed side chains of the C-terminal domain show weak interactions within these eye lens extracts, which are missing for the E107A variant.

This work was performed as part of project A08 of the Collaborative Research Centre Transregio CRC-TRR 102 "Polymers under multiple constraints" and is part of this special issue of Macromolecular Bioscience, which represents the final report of this research network. Our overall goal in project A08 was to investigate the stability of the eye-lens crystallin mixture against different stimuli, also considering crowding conditions. Along these lines, we confirmed that α-crystallin, a large polydisperse multimer, acts as hard-sphere colloid with minimized interactions and almost unconstrained rotational diffusion.[18,19] Notably, this behavior is distinct from many other proteins, which usually show a strong degree of rotational-translational coupling upon crowding.[20] We also established low-resolution ^{1}H NMR relaxometry as a simple tool to monitor aggregation under crowding conditions,[21,22] showing that highly concentrated γB-crystallin aggregates slowly at 60 °C, while αB-crystallin forms transparent gels. In-depth studies of the latter are underway. β- and γ-crystallins belong to the few examples of globular proteins, which show liquid–liquid phase separation.[1] Along these lines, we found that the C- and N-terminal domains contribute differently to the intermolecular interactions driving LLPS. These finding will be published elsewhere.

2. Results

We employed NMR spectroscopy in order to gain high resolution molecular insights into the soluble fractions of hγD after UV-B exposure. Therefore, we completely assigned the backbone resonances and the aromatic ^{1}H-^{13}C HSQC of hγD and several variants (see the Experimental Section; all experiments with wild type and E107A hγD have been performed with protein without His tag). We could confirm earlier findings that the chemical shifts of various backbone resonances of the N-terminal domain change around the substituted Arg at position W43 (Figure S8, Supporting Information) although the crystal structure of W43R showed only very minor structural rearrangements compared to wild type hγD.[14] By contrast, the E107A substitution significantly changed only the backbone resonances of next neighbor D108 (Figure S9, Supporting Information).

2.1. Modified Aromatic Residues of hγD after UV-B Irradiation

100 μM fully ^{13}C enriched hγD samples were exposed to 100 J cm^{-2} and subsequently analyzed by NMR spectroscopy. A minor fraction (≈10%) of heavily damaged hγD that aggregated during the process was removed by centrifugation and the soluble fraction was analyzed. The ^{1}H-^{15}N HSQC spectra revealed no differences between irradiated and non-irradiated samples (Figure S2, Supporting Information) indicating that the overall structure is not affected by this treatment. Inspection of the aromatic resonances in a constant time ^{1}H-^{13}C HSQC disclosed

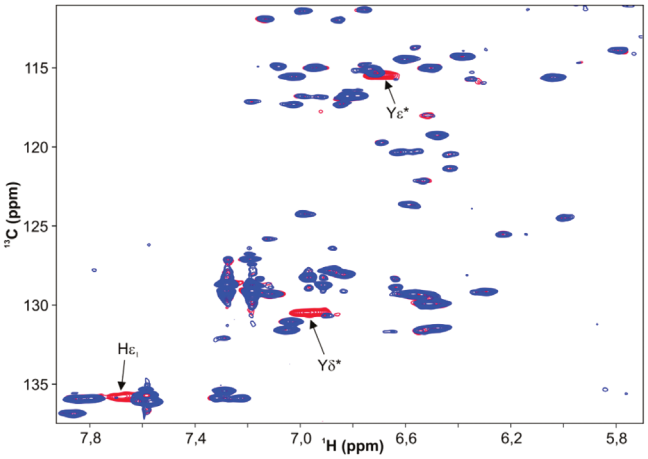

Figure 2. ^{1}H-^{13}C HSQC of aromatic side chains of hγD. Blue contour lines represent hγD before UV-B irradiation and red lines the spectrum after 100 J cm^{-2} irradiation at 310 nm. New cross peaks appear in spectral regions typical for Tyr ϵ*/δ* and His $\epsilon_1$carbons.

three new cross peaks after UV-B treatment not present in the non-irradiated sample (**Figure 2**). They are located in the spectral sections of random coil tyrosine ϵ*/δ* (see spectrum of L-tyrosine in Figure S12, Supporting Information) and histidine ϵ_1 resonances. Since no new random coil signals could be detected for phenylalanines, trytophanes, and most aliphatic resonances, we can rule out a global unfolding of the protein. This is in agreement with the observations for the backbone and side chain amides in the ^{1}H-^{15}N HSQC. At this stage we can conclude that we observe a rather local UV-B induced unfolding involving tyrosines and histidines. The overall pattern does not change over time showing there is no equilibrium between the native and the UV-B altered state suggesting that the local unfolding is caused by a chemical modification of the protein. Since we can observe typical resonances for histidine and tyrosine, we know that it is not these side chains that are chemically modified. A closer look to the long-term behavior of the UV-B induced modification by recording ^{1}H-^{13}C HSQC spectra up to 4.5 months after irradiation (Figure S4, Supporting Information) shows that the intensity of the new cross peaks dropped down to stable values between 20% and 40% after this time and the broad line widths observed directly after irradiation reduced to the typical values of the other aromatic resonances, which were not affected by UV-B. Again, all other cross peaks did not change in intensity or line width during these 4.5 months.

We were unable to directly identify the Tyr and His residues causing the new signals since no aromatic cross peaks showed a significant drop in intensity after UV-B exposure (Figure S3, Supporting Information).

2.2. Identification of UV-B Modified Aromatic Residues of hγD

Since a straight forward NMR spectral identification of modified aromatic hγD side chains after UV-B irradiation causing the three additional cross peaks shown in Figure 2 was not possible we approached their identification indirectly by mutational studies. We irradiated the sole N- and C-terminal domain and residue substituted full-length hγD. Inspection of the ^{1}H-^{13}C HSQC spectra of the separated domains (Figure S6, Supporting Information) showed the same additional cross peaks in regions for Tyr ϵ*/δ* nuclei for the N-terminal but not for the C-terminal domain. An assignment of the additional histidine cross peak to one of both domains was not possible because of a strong spectral overlap with histidines from the His tag. At this stage we know, that the tyrosine and histidine residues causing the additional UV-B induced signals are located in the N-terminal domain.

We suspected Tyr 17, Tyr 29, and His 23 (**Figure 3**A) to be the residues causing the additional signals. This cluster contains the amino acids of interest and is located on the surface, and therefore could unfold locally. Moreover Cys 19 is known to become oxidized upon UV irradiation.[7] We studied the suspected cluster by Y17A, Y29A, and Y17AY29A variants with and without UV-B irradiation by ^{1}H-^{13}C HSQC spectra (Figure 3B). In case of Y17A the same additional cross peaks of the Tyr ϵ*/δ* nuclei after irradiation of the wild type is already visible without irradiation, indicating that remaining Tyr 29 might be the primary residue responsible for the additional signal of the wild type after UV-B treatment (Figure 3B left). In this case, the missing Tyr 17 puts Tyr 29 in a locally unfolded like state. For Y29A hγD we observe a significantly weaker version of the additional Tyr ϵ*/δ* signals after UV irradiation of the wild type (Figure 3B) originating from remaining Tyr 17. As no additional signals after UV irradiation were detected in the double mutant Y17A and Y29A (Figure 3B right) other tyrosines than Y17 and Y29 could be excluded to be involved. In summary we have identified the N-terminal residues responsible for the additional signals with random coil chemical shifts after UV irradiation to be Y17 with a lower contribution and Y29 with a higher contribution. The most likely modified histidine is H23, because it is located in direct neighborhood to Y17, Y29, and C19.

2.3. The Role of W43, W69, and E107 during UV-B Irradiation of hγD

For a more comprehensive insight into UV-B effects on the aromatic cluster of the N-terminal hγD domain, we investigated the W43R and W69A variants by applied the same UV-B treatment as for the wild type. Although the W43R variant had been reported to be thermodynamically less stable and more susceptible to UV damage,[15] none of the amides showed significant changes of the NMR resonances in ^{1}H-^{15}N HSQC spectra (data not shown). The latter also holds for the W69A variant.

The ^{1}H-^{13}C HSQC of the aromatic spectral region of W43R (blue in **Figure 4** middle) showed signals similar to the UV-B irradiated wild type (red in Figure 4 left) already without irradiation. Therefore, the above discussed aromatic cluster (Figure 3A) is already locally unfolded by the close by W43R mutation. By contrast, the more distant W69A substitution only showed additional cross peaks for Tyr ϵ*/δ* nuclei at the same chemical shifts as the wild type after irradiation (red in Figure 4 right). This indicates the outstanding role of W43 not only for the global stability of hγD but also the local folding of the N-terminal Tyr cluster.

The hereditary E107A variant was found in the eye lens core of infants developing cataract.[17] Our NMR assignments of the backbone resonances showed only very local differences com-

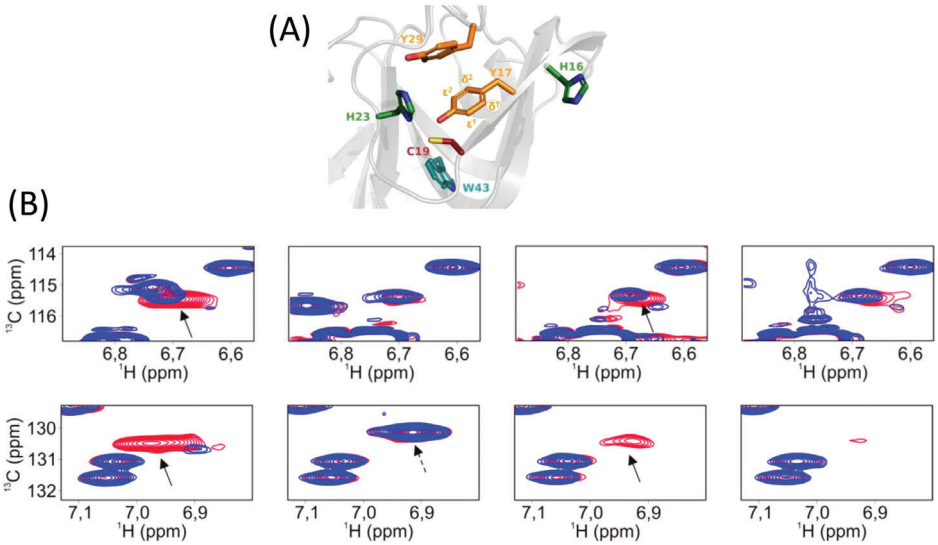

Figure 3. ^{1}H-^{13}C HSQC of aromatic side chains of UV-B irradiated hγD variants. A) Structural representation of the aromatic cluster of the N-terminal domain (2klj.pdb). B) Blue contour lines represent hγD and its Y17A, Y29A, and Y17AY29A variants before and red lines after UV-B irradiation.

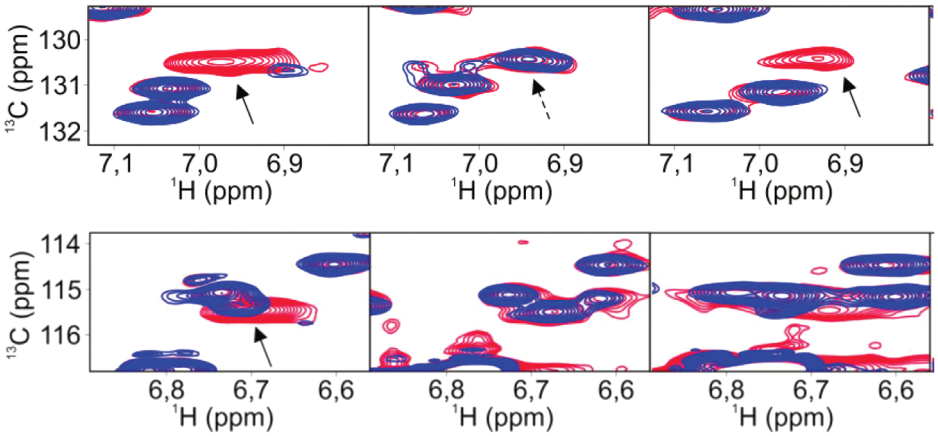

Figure 4. ^{1}H-^{13}C HSQC of aromatic side chains of UV-B irradiated W43R and W69A hγD variants. Blue contour lines represent hγD and its variants before and red lines the after UV-B irradiation.

pared to the wild type protein (Figure S9, Supporting Information). This confirms an earlier study with almost identical far-UV CD spectra of wild type and E107A hγD.[16] The same study showed also no difference in the thermodynamic stability of both proteins during temperature- and denaturant-induced unfolding. We confirmed the latter two observations for our preparations of hγD and its E107A variant (Figure S10, Supporting Information). However, E107A hγD was more susceptible to UV-B irradiation damage compared to the wild type and the so far described variants. Some backbone amide resonances show chemical shift changes and many signal intensities deviated after UV-B treatment in both the N-terminal and C-terminal domains (Figure S11, Supporting Information), indicating more global modifications. The resonances of the aromatic residues showed the same additional cross peaks for the Tyr ϵ^*/δ^* and His ϵ_1 nuclei (black headed arrows in **Figure 5**) plus various addition signals (open headed arrows in Figure 5) close to the random coil values of aromatic side chains. After one month, the very broad Tyr ϵ^*/δ^* signals disappeared to some extend and sharper resonances appeared very close to the chemical shifts of the sole amino acid L-tyrosine (Figure S12, Supporting Information) indicating the progression toward a denatured aromatic N-terminal cluster.

2.4. Fluorescence Properties of hγD and Variants after UV-B Treatment

Further insights into the contribution of individual aromatic side chains of hγD during energy dissipation can be derived by substitution of individual residues and subsequent recording of the intrinsic tryptophan fluorescence after excitation at 300 nm. As expected from earlier studies,[8,14] the W43R substitution reduces the intensity of fluorescence emission by ≈50% because the energy transfer from W43 to W69 is missing and thus only directly exited W69 will emit (**Figure 6**). The W131A substitution in the C-terminal domain has the same but less pronounced

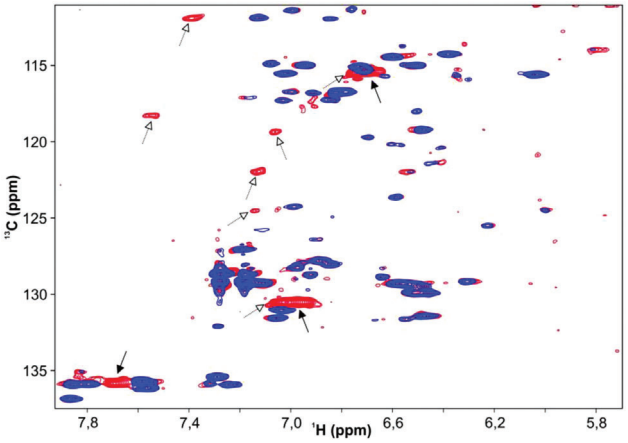

Figure 5. ^{1}H-^{13}C HSQC of aromatic side chains of UV-B irradiated E107A hγD. Blue contour lines represent E107A hγD before and red lines after UV-B irradiation. Additional cross peaks also observed for wild type hγD are indicated by black arrows, further new cross peaks by white arrows.

effect. Note, that there is no significant energy transfer between N- and C-terminus.[9] Correspondingly, alanine substitutions of the energy transfer acceptors W69 and W157 increases the fluorescence emission up to ≈150% because of the missing energy transfer from the donor tryptophanes. Fluorescence emission of the Y17A, Y29A, and E107A variants correspond to wild type hγD.

To follow possible modifications upon UV-B treatment of 100 J cm^{-2}, fluorescence spectra were also recorded after this irradiation. Note, that above 295 nm tryptophan residues are the only naturally occurring protein side chains with a significant extinction coefficient. The amount of aggregated protein (up to 10%) of hγD after UV-B treatment varied substantially between each preparation and for the different variants. Therefore, the concentration of the supernatant after centrifugation of each preparation was adjusted to 120 μM to allow comparisons between the different fluorescence spectra. Wild type, W43R, Y17A, Y29A, and E107A hγD showed not significant and W69A, W131A, and W157A slightly reduced fluorescence emission after the UV-B treatment. This indicates that none of the tryptophan residues got substantially modified during the photoprotective energy transfer (Figure 6) in agreement with observation of the NMR spectra.

2.5. Recombinant hγD in Cataract Eye Lens Extracts

Heteronuclear NMR spectroscopy allows to follow individual, isotope-labeled proteins in their natural cellular environment because resonances of the nonlabeled compounds can by filtered out. This is the basis of in cell NMR spectroscopy.[23,24] We applied the same principle by adding eye lens extracts derived from cataract surgery patients to fully ^{15}N^{13}C labeled recombinant 100 and 250 μM hγD samples. The added protein content of the extracts was ≈15 mg mL^{-1} which corresponds to ratios of ≈1:8 and 1:3, respectively. Note that the lens extracts contain endogenous hγD. Size exclusion chromatography of these extracts showed, as expected from age-related cataract,[25] that the α-crystallin content was reduced by more than 50% (Figure S7, Supporting Information) compared to the literature value of nonpathological eye lenses.[26]

The amide chemical shifts of hγD in ^{1}H-^{15}N HSQC spectra in the absence and presence of the eye lens extracts were identical (**Figure 7**A) indicating that there are only very weak interactions between the recombinant hγD and the α-, β-, and γ-crystallins from the eye lens, which could not induce any conformational change. The same holds for the general line shape of the resonances in these spectra indicating that the overall rotations correlation time of hγD is hardly affected. The only indication for these weak interactions are the cross peak intensities, were some residues showed intensity changes just above the general scatter; most of those are located in the C-terminal domain of hγD (Figure 7B). All of the thus identified backbone amides carried side chains, which are exposed to the surface. We performed exactly the same experiment with the E107A variant (Figure 7C), where the cluster of weak interacting residues in the C-terminus was not present.

Next, we supplemented the eye lens extracts with 800 μM recombinant αB crystallin to reach the α crystallin content of nonpathological eye lens extracts reported in the literature (Figure S13, Supporting Information).[26] Analysis of the backbone resonances of the added recombinant and isotope labeled hγD revealed for the wild type and the E107A variant now also weak interactions with the N-terminal domain (Figure S14, Supporting Information), which we assign to the increased amount of αB-crystallin in the eye lens extracts. The difference between both proteins concerning the C-terminus was not affected.

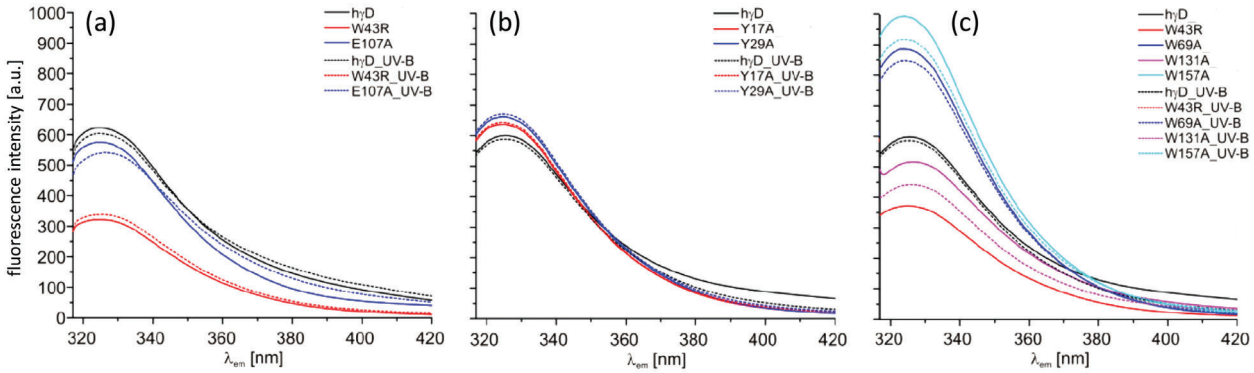

Figure 6. Fluorescence emission spectra of hγD and variants. Solid lines represent the spectrum after excitation at 295 nm before and dotted lines after UV-B treatment. Protein concentrations were kept constant for all experiments for a direct comparison. A) hγD wild type, W43R, and E107A variant, B) hγD wild type, Y17A, and Y29A variant, and C) hγD wild type, W69A, W131A, and W157A variant are compared.

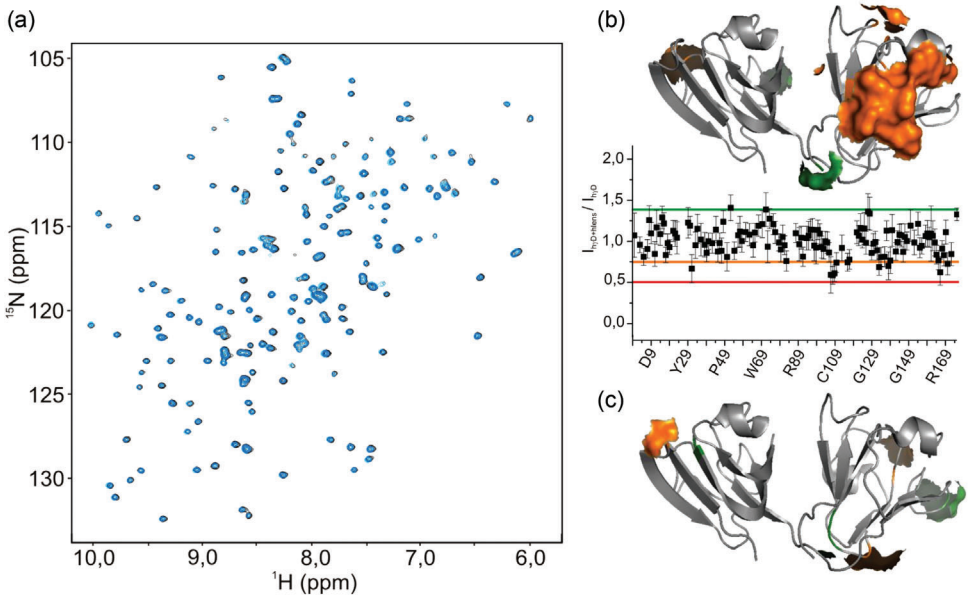

Figure 7. ^{1}H-^{15}N HSQC of hγD in eye lens extracts from cataract patients. A) ^{1}H-^{15}N HSQC spectra of 100 μM hγD in (black) the absence and (blue) the presence of 15 mg mL^{-1} eye lens extracts at 37 °C. B) Cross peak intensity ratios of the backbone amides. These ratios were normalized to the average over all ratios and color coded in green for values above 1.35, in orange for values below 0.75, in red for values below 0.5 and mapped on the hγD structure (2klj.pdb). C) Analogous mapping approach for E107A hγD.

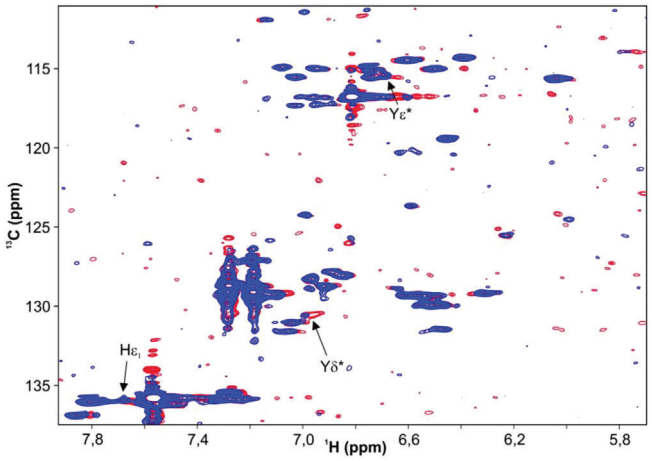

Figure 8. ^{1}H-^{13}C HSQC of aromatic side chains of UV-B treated hγD in eye lens extracts. Blue contour lines represent 250 μM hγD in 15 mg mL^{-1} eye lens extracts before UV-B irradiation and red lines the spectrum after 100 J cm^{-2} irradiation at 310 nm. Arrows indicate the Tyr ϵ^*/δ^* and His ϵ_1 cross peaks identified in the absence of eye lens extracts which have here lower intensities.

2.6. Reduced UV-B Induced hγD Modification in Eye Lens Extracts

Finally, the mixture of recombinant ^{15}N^{13}C hγD and the eye lens extracts from cataract patients were exposed to the same dose of UV-B as wild type and the hγD variants described above. The ^{1}H–^{15}H correlation spectrum again showed no significant spectral changes (data not shown). The ^{1}H-^{13}C HSQC of the aromatic side chains (**Figure 8**) revealed again the two additional cross peaks for the Tyr ϵ^*/δ^* nuclei already observed for hγD in the absence of eye lens extracts but with much reduced intensity. The signal-to-noise ratio of this complex NMR sample was not sufficient for a statement about the earlier observed additional His ϵ_1 cross peak. Together, this indicates that the threefold excess of eye lens crystallins from cataract patients remained photoprotective to some extent.

3. Discussion

The protein composition of the human eye lens prevents damage of the retina by filtering out UV-B from the focused light beam. γD-crystallin facilitates here energy dissipation by fluorescence resonance energy transfer between aromatic side chains.[8,9,27] Although these processes are very effective, protein damages caused by the intermediate high energy states occur and accumulate because of a missing turnover of the lens proteins during human lifetime. The estimated ambient UV-B irradiation entering the eye lens with a hγD concentration in the millimolar range over 70 years is ≈2.3 J cm^{-2}.[5] In this study, we used 100 J cm^{-2} of 100–250 μM hγD samples without further analyzing the up to 10% aggregated and removed protein. According to literature, these aggregates contain covalent and oxidized species.[1,7]

With the here presented experimental approach, we analyzed the UV-B modified γD-crystallin moiety, which remained soluble. Our data suggest that only the N-terminal aromatic cluster next to Cys 19 gets modified leading to a local unfolding of Tyr 17, Tyr 29, and most likely His 23 (Figure 3A). This species was not prone to aggregation for months, but a very slow process within this time range caused an exponential decay of the additional Tyr ϵ^*/δ^* resonances. In other words, local UV damage at the aromatic cluster does not alter the overall properties of hγD. It can be seen as a controlled damage caused by UV without directly causing aggregation. This extends an earlier analysis of UV-B damaged and

aggregated hγD by mass spectrometry suggesting Cys 19 and Tyr 17 as prime residues for radical polymerization.[7]

In the subsequent analyses we used the UV-B induced additional aromatic NMR cross peaks of wild type hγD as spectral read out when analyzing the variants and the more physiologic environment of eye lens extracts. ^{1}H-^{15}N HSQC spectra are the NMR fingerprint for an overall view on the 3D structure of proteins. No significant changes in chemical shifts and signal intensities were detected upon UV-B treatment for wild type hγD and its aromatic side chain substituted variants (Figure S2, Supporting Information). By contrast, it had been reported that cross peak intensities of many backbone amides in ^{1}H-^{15}N HSQCs of the N-terminal domain of hγD decayed by more than 50% after UV-C irradiation at 245 nm mainly caused by damage of W43.[14] The thermodynamically less stable N-terminal domain was more sensitive to UV-C irradiation,[14,28] where doses below 5 J cm^{-2} caused already W43 damage and the corresponding NMR spectral changes of the amides.[14] The observation that the here used 20-fold higher dose caused much less damage shows the very effective energy dissipation of hγD for UV-B light. It should be noted that irradiation of UV light below 280 nm gets completely absorbed by the cornea of the eye, whereas few percent of the here used UV-B at 310 nm can reach the eye lens.[5] So overall, UV-B is causing less damage and the lesser damage is not reflected in the ^{1}H-^{15}N HSQC experiments. It therefore is beneficial to directly look at aromatic side chains in order to observe subtle changes caused by UV-B.

The here presented NMR studies of Trp substitutions suggest that the UV-B induced modification process starts by absorption of W43, which is the subsequent donor of energy transfer to W69 during the natural photoprotective reaction. If W43 is missing, the surface-exposed cluster of the N-terminal domain is locally unfolded and no UV-B modification was observed neither by NMR and nor in the fluorescence emission. If the acceptor W69 is missing, the same NMR detectable modifications around Y17 occur as in the wild type protein. Variants with substitution of W69, W131, or W157 to alanine showed reduced fluorescence emission after UV-B treatment probably because energy dissipation was less efficient and more hγD molecules are modified.

The so far employed NMR read out of UV-B induced modifications could also be used to follow hγD in eye lens extracts. Although we could not reach the millimolar protein concentrations of the intact eye lens because of aggregation during concentrating the eye extracts, a threefold excess of eye lens extracts compared to the recombinant and isotope labeled hγD could reduce, but not fully prevent the UV-B modification. We attribute this effect mainly to the endogenous γ-crystallin fraction in the extracts; further UV-B photoprotective contributions from the α- and β-crystallin fraction are not expected.

The E107A substitution in the C-terminal domain was found in the early onset of cataract of children. We found for this variant the same thermodynamic stability during denaturant induced unfolding at 37 °C and up to 65 °C in heat-induced aggregation as the wild type, thus verifying published results,[16] although this has been challenged by another study reporting a lower stability and increased aggregation properties under different buffer conditions.[29] Other disease related variants differ here such as W43R hγD, which has reduced thermodynamic stability coupled to a higher UV damage susceptibility compared to wild type.[13–15] Further examples include P23T, R37S, and R56H substitutions, which showed wild type stability and very minor structural rearrangements but increased insolubility.[30–32] Our NMR analysis revealed that E107A has no significant impact on the structure. However, the sensitivity for UV-B induced modification in the N-terminal domain increased for the variant and the number of weak interactions of the C-terminal domain with other crystallins in the eye lens decreased compared to the wild type. The E107A substitution increases the isoelectric point of hγD from 7.2 to 8.2 and therefore the surface charge at pH 7, which was one suggested reason for this variant to drive LLPS.[16] This might also explain our observed long-distance effects and modified intermolecular interactions. For the S76A variant, a similar shift in the isoelectric point had been reported,[33] which did not significantly change the structure and stability of hγD but altered interactions with other lens proteins had been suggested.

4. Experimental Section

Expression and Purification of Human γD-Crystallin: hγD and its variants were recombinantly expressed in *Escherichia coli* BL21(DE3) or Rosetta pLyS cells containing the pET14b vector with an N-terminal thrombin cleavage site for the His_6 tag following standard protocols.[34] IPTG induction occurred at OD_{600} between 0.7 and 1.0 in M9 minimal medium containing $^{15}NH_4Cl$ and ^{13}C-glucose or 1–^{13}C glucose or 2–^{13}C glucose as sole source for the respective isotopes. The protein of interest from harvested, centrifuged, and lysed cells was purified by a nickel-NTA column chromatography. Cleavage of the His_6 tag occurred by thrombin for all preparations of wild type and E107A hγD. The W43R, W69A, W131A, Y17A, Y29A, and Y17A/Y29A variants and the single C- and N-terminal domains remained His_6 tagged.

NMR Sample Preparation and Assignment of Aromatic NMR Resonances: NMR samples contained 1.1 mM protein in 50 mM sodium phosphate, 50 mM sodium chloride, 10% D_2O, and 0.02% sodium azide at pH 7.5 and were measured at 25 °C on Bruker Avance III 600 MHz and Avance II 800 MHz spectrometer, the latter equipped with a cryo probe. Spectra were processed and visualized by NMRpipe and NMRviewJ. Only about one half of all NMR resonances of the aromatic side chains of hγD had been assigned so far.[14,35] For complete assignment of the aromatic resonances (Figure S1, Supporting Information) based on the existing backbone assignments (H^N, N, Cα, Cβ)[14,35] (HB)CB(CGCD)HD,[36] aromatic ^{1}H-^{13}C TOCSY-HSQC, and ^{2}J-^{1}H-^{15}N HSQC experiments were used.[37] To reduce complexity and to increase relaxation properties, the assignment was first conducted on the fully ^{13}C/^{15}N labeled N-terminal and C-terminal domains and later transferred to the full length protein. The assignment was further validated by the use of 1–^{13}C glucose or 2–^{13}C glucose as sole carbon source for a selective isotope labeling of individual carbons in Tyr, Phe, Trp, and His residues.[38,39] Remaining ambiguities could be solved by fully assigning the protein variants W43R, W69A, W131A, W157A, Y17A, Y29A, and Y17AY29A and comparison with the wild type spectra.

UV-B Irradiation: 550 µL of 100–250 µM hγD-crystallin samples in a 1.5 mL Eppendorf cap were irradiated at 310 nm by four 20 W lamps till 100 J cm^{-2} had been reached. About 10% of the protein aggregated during irradiation, which was removed by centrifugation and not further analyzed.

Fluorescence Spectroscopy: Fluorescence spectra between 310 and 420 nm of hγD and variants were recorded with 1–3 µM samples at 25 °C after excitation at 300 nm and a band width of 10 nm in a Jasco FP-6500 spectrometer. The concentration of soluble protein after UV treatment was adjusted to 120 µM before dilution.

Eye Lens Extracts: Extracts from human eye lenses were derived from the University Clinic and Polyclinic for Ophthalmology in Halle from cataract patients who underwent a surgery to remove the eye lens by phacoemulsification. Anonymous rendered extracts were collected and stored in physiological sodium chloride at −20 °C. The Ethic Commission of the Medical Faculty of the Martin Luther University Halle-Wittenberg has ap-

proved practice (Approval Number 2014–162). For the NMR experiments, the extracts were sixfold diluted to reach 50 mM sodium phosphate, 1 mM EDTA, 0.2 mM DTT, and 0.02% sodium azide at pH 7.5 and stirred at 4 °C to dissolve the protein fraction. The supernatant after centrifugation at 48 000 × *g*, was concentrated with Amicon ultra centrifugal filters and dialyzed against 50 mM sodium phosphate, 50 mM sodium chloride, and 1 mM EDTA at pH 7.5. α-, β-, and γ-crystallin fractions were analyzed by size exclusion chromatography using a Superdex 200 HiLoad 16/600 column. NMR samples contained 100 µm isotope labeled hγD and 15 mg mL^{-1} eye lens extracts. Higher concentrations could not be achieved without aggregation probably because of the strongly reduced content of α-crystallin. Addition of recombinant α crystallin up to the ratio of nonpathological values[26] did not help to overcome this aggregation limit.

Supporting Information

Supporting Information is available from the Wiley Online Library or from the author.

Acknowledgements

The authors are grateful to Erik Chankiewitz from the University Clinic and Polyclinic for Ophthalmology in Halle for providing eye lens extracts from cataract patients, Andrea Sinz and co-workers for providing their equipment for UV-B irradiation of protein samples, and Katrin Waldheim for purification of Y17AY29A hγD. This work was funded by the Deutsche Forschungsgemeinschaft (DFG, Project No. 189853844 – TRR 102, TP A08). The European Regional Development Fund (ERDF) of the European Union is acknowledged for partially funding of the NMR facility of the Martin-Luther-University.

Open access funding enabled and organized by Projekt DEAL.

Conflict of Interest

The authors declare no conflict of interest.

Data Availability Statement

The data that support the findings of this study are available from the corresponding author upon reasonable request.

Keywords

cataract, crystallin, protein NMR, tryptophan fluorescence, UV damage

Received: November 30, 2022
Revised: February 1, 2023
Published online:

[1] M. A. Rocha, M. A. Sprague-Piercy, A. O. Kwok, K. W. Roskamp, R. W. Martin, *ChemBioChem* **2021**, *22*, 1329.
[2] D. S. George, M. H. Ainslie-Garcia, N. C. Ferko, H. Cheng, *Clin. Ophthalmol.* **2021**, *15*, 923.
[3] J. F. Hejtmancik, *Semin. Cell Dev. Biol.* **2008**, *19*, 134.
[4] H. Bloemendal, W. De Jong, R. Jaenicke, N. H. Lubsen, C. Slingsby, A. Tardieu, *Prog. Biophys. Mol. Biol.* **2004**, *86*, 407.
[5] D. H. Sliney, *Int. J. Toxicol.* **2002**, *21*, 501.
[6] D. I. Pattison, A. S. Rahmanto, M. J. Davies, *Photochem. Photobiol. Sci.* **2012**, *11*, 38.
[7] N. Schafheimer, Z. Wang, K. Schey, J. King, *Biochemistry* **2014**, *53*, 979.
[8] J. Chen, S. L. Flaugh, P. R. Callis, J. King, *Biochemistry* **2006**, *45*, 11552.
[9] J. Chen, P. R. Callis, J. King, *Biochemistry* **2009**, *48*, 3708.
[10] N. Braun, M. Zacharias, J. Peschek, A. Kastenmüller, J. Zou, M. Hanzlik, M. Haslbeck, J. Rappsilber, J. Buchner, S. Weinkauf, *Proc. Natl. Acad. Sci. USA* **2011**, *108*, 20491.
[11] B. C. Searle, S. Dasari, P. A. Wilmarth, M. Turner, A. P. Reddy, L. L. David, S. R. Nagalla, *J. Proteome Res.* **2005**, *4*, 546.
[12] E. Serebryany, J. C. Woodard, B. V. Adkar, M. Shabab, J. A. King, E. I. Shakhnovich, *J. Biol. Chem.* **2016**, *291*, 19172.
[13] E. Serebryany, S. Yu, S. A. Trauger, B. Budnik, E. I. Shakhnovich, *J. Biol. Chem.* **2018**, *293*, 17997.
[14] F. Ji, J. Jung, L. M. I. Koharudin, A. M. Gronenborn, *J. Biol. Chem.* **2013**, *288*, 99.
[15] B. Wang, C. Yu, Y.-B. Xi, H.-C. Cai, J. Wang, S. Zhou, S. Zhou, Y. Wu, Y.-B. Yan, X. Ma, L. Xie, *Hum. Mutat.* **2011**, *32*, E1939.
[16] P. R. Banerjee, A. Pande, J. Patrosz, G. M. Thurston, J. Pande, *Proc. Natl. Acad. Sci. USA* **2011**, *108*, 574.
[17] O. M. Messina-Baas, L. M. Gonzalez-Huerta, S. A. Cuevas-Covarrubias, *Mol. Vision* **2006**, *12*, 995.
[18] G. Foffi, G. Savin, S. Bucciarelli, N. Dorsaz, G. M. Thurston, A. Stradner, P. Schurtenberger, *Proc. Natl. Acad. Sci. USA* **2014**, *111*, 16748.
[19] M. Roos, S. Link, J. Balbach, A. Krushelnitsky, K. Saalwächter, *Biophys. J.* **2015**, *108*, 98.
[20] M. Roos, M. Ott, M. Hofmann, S. Link, E. Rössler, J. Balbach, A. Krushelnitsky, K. Saalwächter, *J. Am. Chem. Soc.* **2016**, *138*, 10365.
[21] M. Camilles, S. Link, J. Balbach, K. Saalwachter, A. Krushelnitsky, *Biochim. Biophys. Acta, Proteins Proteomics* **2018**, *1866*, 1055.
[22] M. Camilles, S. Link, J. Balbach, K. Saalwächter, A. Krushelnitsky, *Biochim. Biophys. Acta, Proteins Proteomics* **2019**, *1867*, 453.
[23] A. Kumar, L. T. Kuhn, J. Balbach, *Int. J. Mol. Sci.* **2019**, *20*, E378.
[24] P. Selenko, D. P. Frueh, S. J. Elsaesser, W. Haas, S. P. Gygi, G. Wagner, *Nat. Struct. Mol. Biol.* **2008**, *15*, 321.
[25] J. Horwitz, M. P. Bova, L.-L. Ding, D. A. Haley, P. L. Stewart, *Eye* **1999**, *13*, 403.
[26] L. R. Miesbauer, X. Zhou, Z. Yang, Z. Yang, Y. Sun, D. L. Smith, J. B. Smith, *J. Biol. Chem.* **1994**, *269*, 12494.
[27] J. Chen, D. Toptygin, L. Brand, J. King, *Biochemistry* **2008**, *47*, 10705.
[28] M. S. Kosinski-Collins, S. L. Flaugh, J. King, *Protein Sci.* **2004**, *13*, 2223.
[29] N. Asherie, J. Pande, A. Pande, J. A. Zarutskie, J. Lomakin, A. Lomakin, O. Ogun, L. J. Stern, J. King, G. B. Benedek, *J. Mol. Biol.* **2001**, *314*, 663.
[30] A. Basak, O. Bateman, C. Slingsby, A. Pande, N. Asherie, O. Ogun, G. B. Benedek, J. Pande, *J. Mol. Biol.* **2003**, *328*, 1137.
[31] J. C. Boatz, M. J. Whitley, M. Li, A. M. Gronenborn, P. C. A. Van Der Wel, *Nat. Commun.* **2017**, *8*, 15137.
[32] A. Pande, J. Pande, N. Asherie, A. Lomakin, O. Ogun, J. King, G. B. Benedek, *Proc. Natl. Acad. Sci. USA* **2001**, *98*, 6116.
[33] F. Ji, J. Jung, A. M. Gronenborn, *Biochemistry* **2012**, *51*, 2588.
[34] T. Gruber, J. Balbach, *PLoS One* **2015**, *10*, 0136922.
[35] J. Jung, I.-J. L. Byeon, Y. Wang, J. King, A. M. Gronenborn, *Biochemistry* **2009**, *48*, 2597.
[36] T. Yamazaki, J. D. Forman-Kay, L. E. Kay, *J. Am. Chem. Soc.* **1993**, *115*, 11054.
[37] J. G. Pelton, D. A. Torchia, N. D. Meadow, S. Roseman, *Protein Sci.* **1993**, *2*, 543.
[38] P. Lundström, K. Teilum, T. Carstensen, I. Bezsonova, S. Wiesner, D. F. Hansen, T. L. Religa, M. Akke, L. E. Kay, *J. Biomol. NMR* **2007**, *38*, 199.
[39] U. Weininger, *Methods Enzymol.* **2019**, *614*, 67.